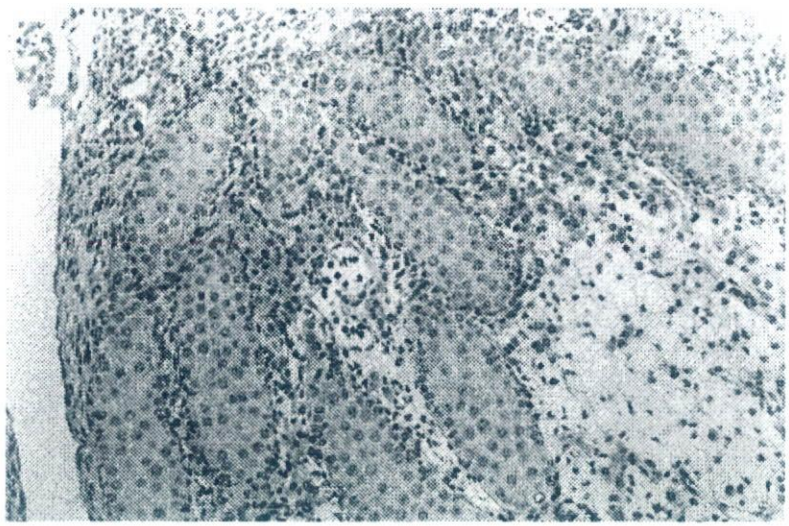

**Photo 2-a.** Testis of a G18 rat fetus from the control group. HE stain, ×160.

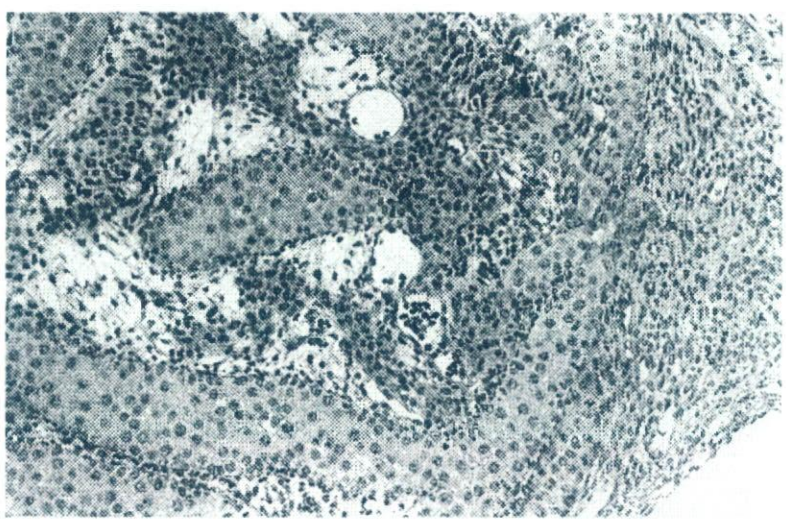

**Photo 2-b.** Testis of a G18 fetus from a rat treated with 500 mg/kg of DEHP showing hyperplasia of interstitial cells. HE stain, ×160.

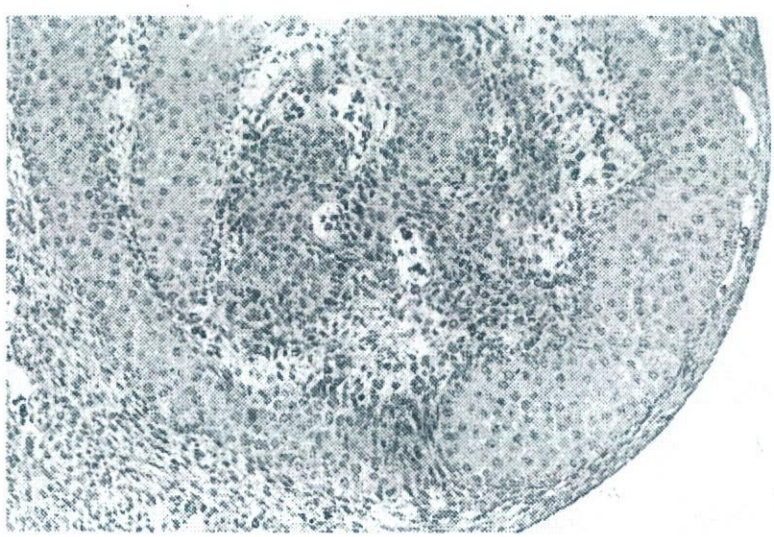

**Photo 2-c.** Testis of a G18 fetus from a rat treated with 1000 mg/kg DEHP showing hyperplasia of interstitial cells. HE stain, ×160.

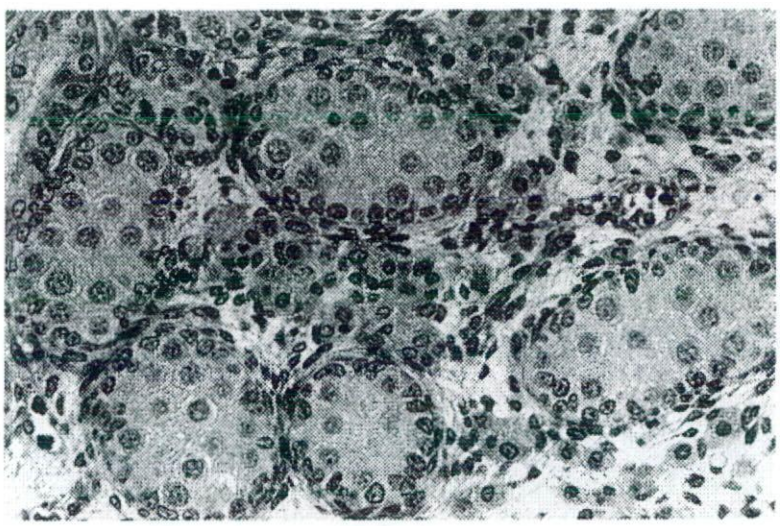

**Photo 3-a.** Testis of a G20 fetus from the control group showing the seminiferous cords and interstitial cells. HE stain, ×310.

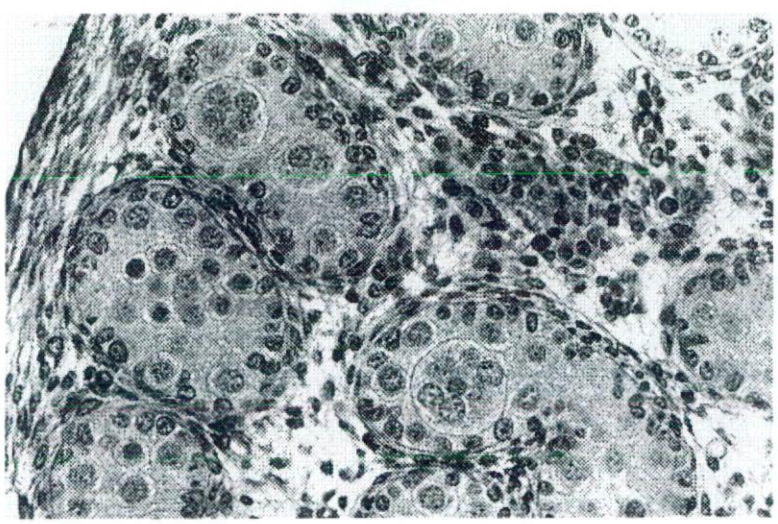

**Photo 3-b.** Testis of a G20 fetus from the group treated with 500 mg/kg of DEHP showing multinucleated germ cells in seminiferous cords. HE stain, ×310.

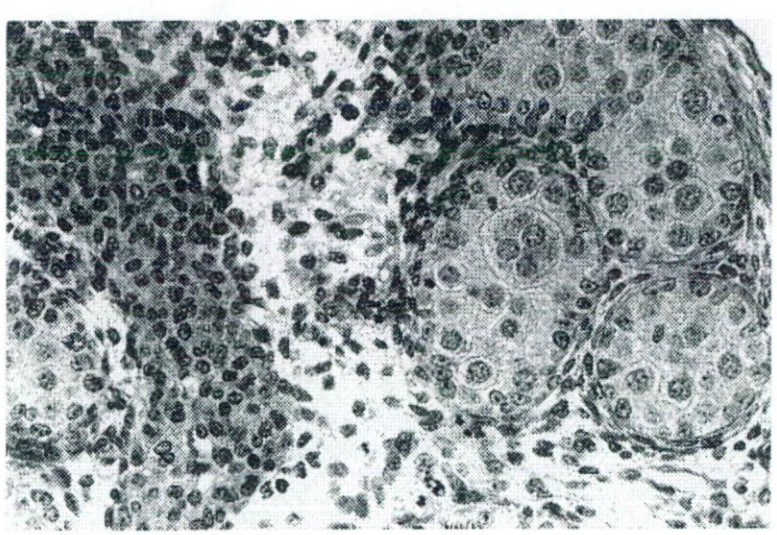

**Photo 3-c.** Testis of a G20 fetus from the group treated with 1000 mg/kg of DEHP showing multinucleated germ cells in seminiferous cords, and hyperplastic smaller-sized interstitial cells. HE stain, ×310.

5a, 5b). In their epididymides, atrophy was found in all of the animals and cell debris in the epididymal lumen was also found (Photos 6a, 6b).

Effects of the lower doses of DEHP on testicular development were examined in Experiment 2. Table 6 summarizes histopathological findings of fetal testes on G20 and testes of offspring at 5 and 10 weeks of age in Experiment 2. Multinucleated germ cells were found in the fetal testes of all the groups exposed to DEHP, although its incidence was very low in the 125 mg/kg group. In the groups exposed to 250 mg/kg and 500 mg/kg of DEHP, partly thickened germinal cords due to aggregation of increased number of germ cells and hyperplasia of the interstitial cells were observed. Degenerated germ cells and apoptosis were observed in a few animals in the group exposed to 500 mg/kg of DEHP. These findings are comparable to those in DEHP-exposed testes at the same dose in Experiment 1.

In contrast to the findings of the fetal testes, no abnormalities were found in testes of the offspring at 5 and 10 weeks of age in any group in histopathological examination. Furthermore, the seminiferous cycles in the testis determined at 5 weeks of age were comparable between control and DEHP-exposed groups (Table 7).

**Electron microscopic findings of fetuses**

Electron microscopic examination of fetal testes was performed in Experiment 1. In the fetal testis of the groups exposed to DEHP at 500 and 1000 mg/kg, degenerated germ cells were found in the testicular cord on G16 (Photo 7), and smaller-sized interstitial cells containing fewer lipid droplets were noted on G18 (Photo 8a). These changes of the interstitial cells became more obvious on G20 (Photo 8b).

In the fetal testis from the group exposed to EE at 0.5 mg/kg, degeneration of germ cells was found only on G14. No abnormalities such as those observed with DEHP treatment were found on G16, 18 and 20. Slightly swollen mitochondria and hyperplastic smooth endoplasmic reticulum were noted in interstitial cells on G18 and 20. Furthermore, degeneration of interstitial cells surrounded by neutrophils infiltration were observed on G20.

In examination of offspring at 5 and 10 weeks after birth in Experiment 2, ultrastructural changes were not observed in the testis and epididymides of any

**Table 5.** Histopathological findings in the testis and epididymis of offspring exposed to DEHP during gestational days 7-18 (Experiment 1) 7 weeks after birth.

| Group | DEHP 500 mg/kg (6) | | | | | DEHP 1000 mg/kg (12) | | | | |
|---|---|---|---|---|---|---|---|---|---|---|
| Grade | − | ± | + | ++ | +++ | − | ± | + | ++ | +++ |
| Testis | | | | | | | | | | |
| Atrophy of seminiferous tubules | 6 | 0 | 0 | 0 | 0 | 2 | 2 | 4 | 3 | 1 |
| Multinucleated giant cells | 5 | 1 | 0 | 0 | 0 | 0 | 3 | 5 | 4 | 0 |
| Dilatation of seminiferous tubules | 6 | 0 | 0 | 0 | 0 | 2 | 0 | 4 | 6 | 0 |
| Dilatation of rete testis | 6 | 0 | 0 | 0 | 0 | 8 | 2 | 1 | 1 | 0 |
| Hyperplasia of interstitial cells | 6 | 0 | 0 | 0 | 0 | 10 | 1 | 1 | 0 | 0 |
| Necrosis | 6 | 0 | 0 | 0 | 0 | 11 | 0 | 0 | 0 | 1 |
| Mineralization | 6 | 0 | 0 | 0 | 0 | 10 | 0 | 1 | 1 | 0 |
| Foreign body giant cells | 6 | 0 | 0 | 0 | 0 | 10 | 0 | 1 | 1 | 0 |
| Focal loss of seminiferous tubules | 6 | 0 | 0 | 0 | 0 | 11 | 0 | 1 | 0 | 0 |
| Malformation of seminiferous tubules | 6 | 0 | 0 | 0 | 0 | 11 | 0 | 1 | 0 | 0 |
| Epididymis | | | | | | | | | | |
| Atrophy | 6 | 0 | 0 | 0 | 0 | 0 | 1 | 2 | 2 | 7 |
| Cell debris in lumens | 0 | 0 | 6 | 0 | 0 | 3 | 3 | 6 | 0 | 0 |
| Dilatation of lumens | 6 | 0 | 0 | 0 | 0 | 8 | 0 | 3 | 1 | 0 |
| Infiltration of lymphocytes | 6 | 0 | 0 | 0 | 0 | 8 | 2 | 2 | 0 | 0 |
| Granuloma | 6 | 0 | 0 | 0 | 0 | 11 | 0 | 0 | 1 | 0 |

Figures in parentheses indicate number of offspring examined.
− : not observed, ± : very slight, + : slight, ++ : moderate, +++ : severe.

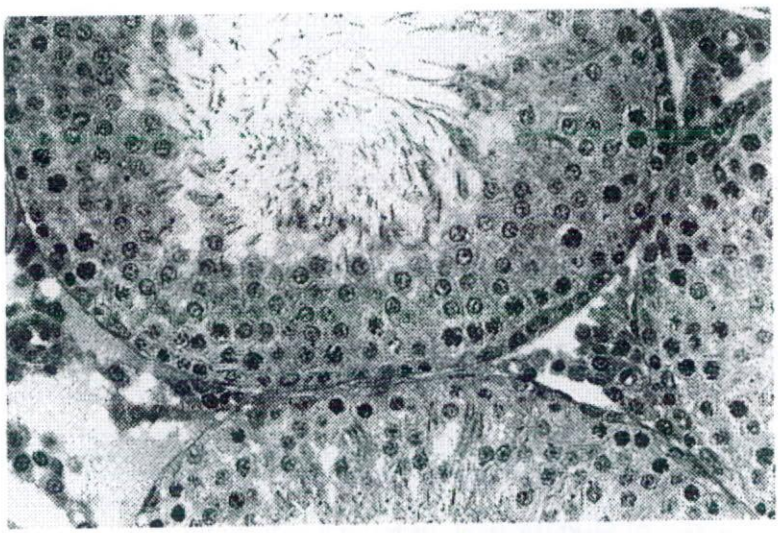

**Photo 4-a.** Testis of a 7-week-old rat treated with 500 mg/kg of DEHP *in utero* showing no abnormalities in the seminiferous tubules and interstitial cells. HE stain, ×310.

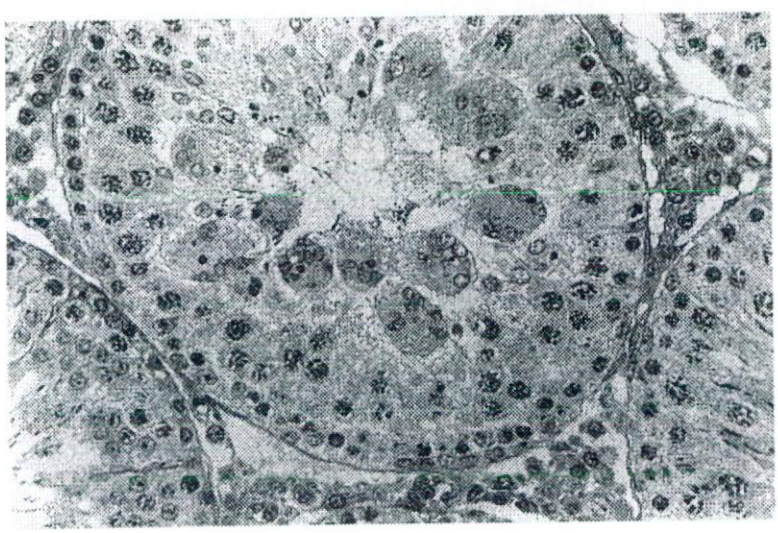

**Photo 4-b.** Testis of a rat of the same group as Photo 4-a, showing multinucleated giant cells in a seminiferous tubule. HE stain, ×310.

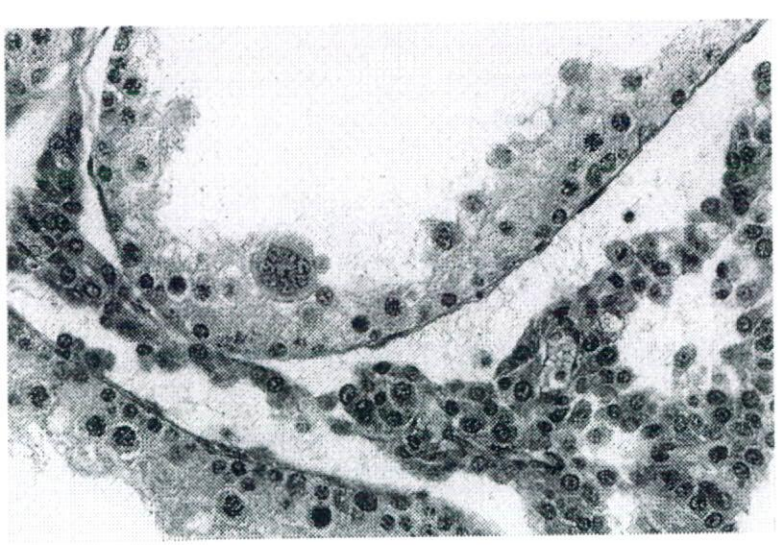

**Photo 4-c.** Testis of a 7-week-old rat treated with 1000 mg/kg of DEHP *in utero*, showing atrophy of seminiferous tubule epithelia with multinucleated giant cell in the lumen, and also hyperplasia of interstitial cells. HE stain, ×310.

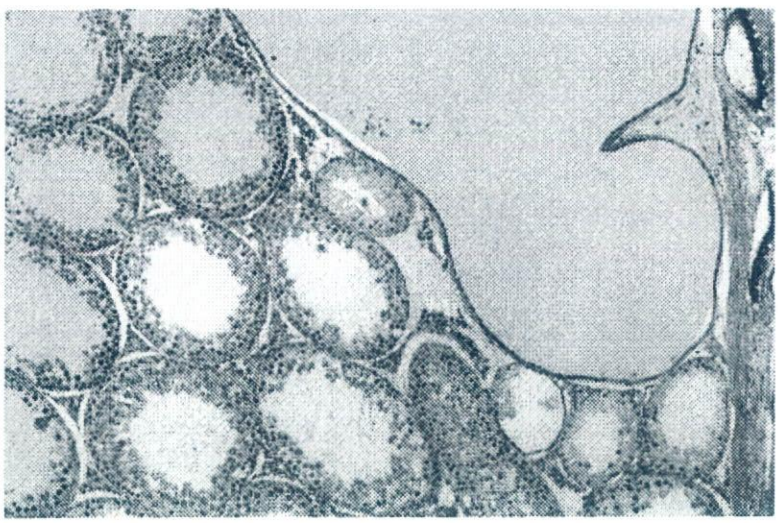

**Photo 5-a.** Testis of a 7-week-old rat treated with 1000 mg/kg of DEHP *in utero*, showing dilatation of seminiferous tubules and of rete testis. HE stain, ×80.

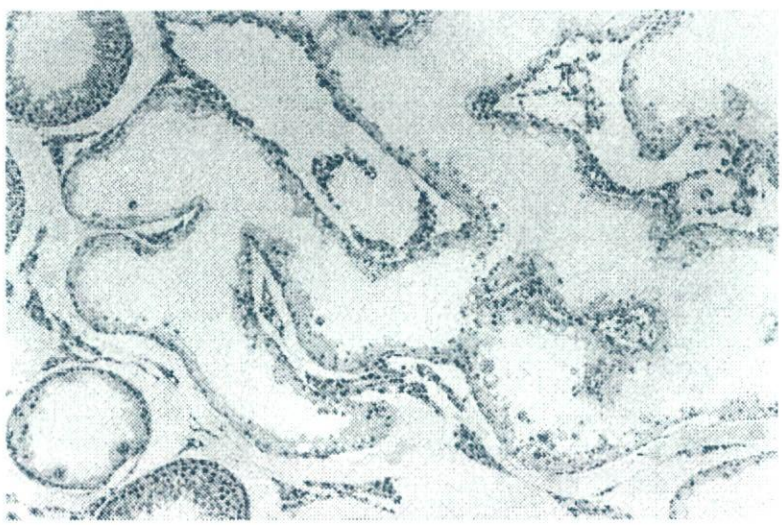

**Photo 5-b.** Testis from a 7-week-old rat treated with 1000 mg/kg of DEHP *in utero*, showing branching of atrophic seminiferous tubules. HE stain, ×80.

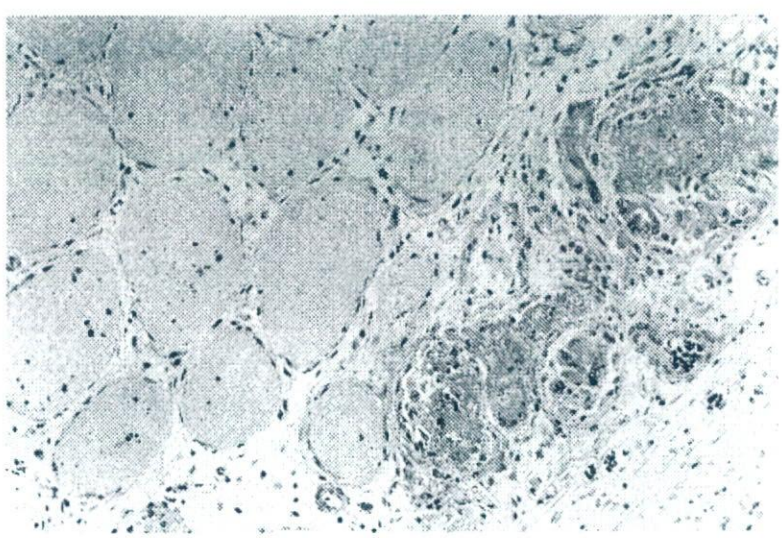

**Photo 5-c.** Testis of a 7-week-old rat treated with 1000 mg/kg of DEHP *in utero*, showing extensive necrosis and foreign body giant cells. HE stain, ×160.

of the offspring in any groups (control and 500 mg/kg DEHP groups).

**Expression of androgen receptors**

Immunohistochemical staining revealed an increase of androgen receptor-positive cells, namely hyperplasia of Leidig cells, in the interstitium of fetal testes at G20 in the 500 mg/kg group (Photo 9). In the offspring at 5 and at 10 weeks after birth, however, the expression of androgen receptors observed in Sertoli cells, myoid cells and interstitial cells was not different among the control and DEHP treated groups (data not shown).

**Examination of sperms**

Sperms collected from the cauda epididymidis of 10-week old offspring were subjected to examination of motility and morphology of the spermatozoa. Results are shown in Table 8. Sperm count and sperm motility were not significantly different between the control and any of the groups treated with DEHP at 125, 250 or 500 mg/kg. There were no remarkable changes in spermatogenic parameters related to treatment.

## DISCUSSION

Oral administration of DEHP to pregnant rats at doses up to 1000 mg/kg from G7 to G18, which corre-

**Photo 6-a.** Epididymis of a 7-week old rat treated with 1000 mg/kg of DEHP *in utero*, showing atrophy of epididymal ducts and cell debris in the lumen. HE stain, ×80.

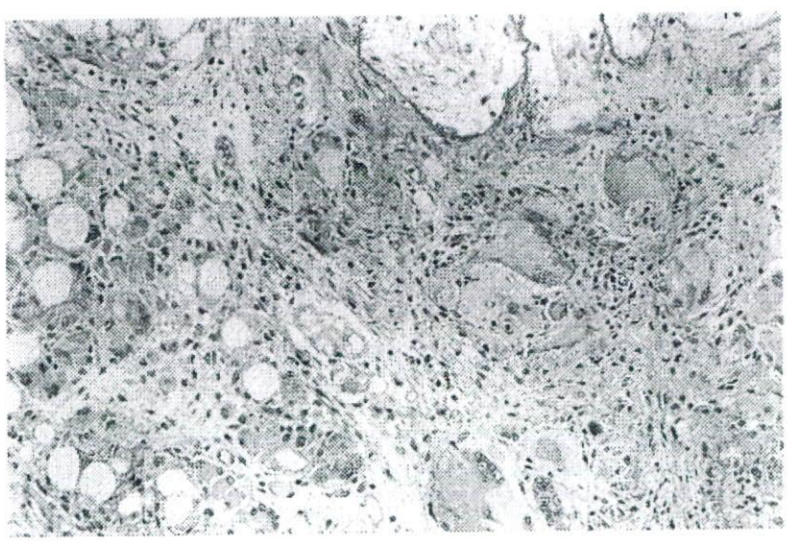

**Photo 6-b.** Granuloma formed in the epididymis of a 7-week-old rat treated with 1000 mg/kg of DEHP *in utero*, accompanied by numerous foreign body giant cells and fibrosis. HE stain, ×160.

sponded to the organogenetic period of a rat fetus, induced fetal damage such as increase in fetal mortality, inhibition of fetal weight gain, and some malformations in the highest dose. Histopathological studies revealed degeneration of germ cells and hyperplasia of interstitial cells in the fetal testis in the groups treated with DEHP at doses of 500 mg/kg and above. Similar changes were also observed in slight degree in the 250 mg/kg group but not in the 125 mg/kg group. Electron microscopic examination of these testes of affected groups revealed smaller-sized interstitial cells in which lipid droplets were depleted. Testicular toxicity of a phthalate ester by *in utero* exposure in rats have been described by Mylchreest *et al.* (2000) using di-(*n*-

**Table 6.** Histopathological findings of testes of offspring exposed to di-(2-ethylhexyl) phthalate (DEHP) during gestational days 7-18 (Experiment 2).

| Group | DEHP 0 mg/kg [a] | | | | | DEHP 125 mg/kg | | | | | DEHP 250 mg/kg | | | | | DEHP 500 mg/kg | | | | |
|---|---|---|---|---|---|---|---|---|---|---|---|---|---|---|---|---|---|---|---|---|
| Grade | – | ± | + | ++ | +++ | – | ± | + | ++ | +++ | – | ± | + | ++ | +++ | – | ± | + | ++ | +++ |
| Gestational day 20 | (15) | | | | | (21) | | | | | (19) | | | | | (28) | | | | |
| Multinucleated germ cells | 15 | 0 | 0 | 0 | 0 | 16 | 5 | 0 | 0 | 0 | 4 | 15 | 0 | 0 | 0 | 2 | 25 | 1 | 0 | 0 |
| Increase of germ cells in a cord | 15 | 0 | 0 | 0 | 0 | 21 | 0 | 0 | 0 | 0 | 16 | 3 | 0 | 0 | 0 | 1 | 21 | 6 | 0 | 0 |
| Hyperplasia of interstitial cells | 15 | 0 | 0 | 0 | 0 | 21 | 0 | 0 | 0 | 0 | 6 | 12 | 1 | 0 | 0 | 6 | 5 | 17 | 0 | 0 |
| Degeneration of germ cells | 15 | 0 | 0 | 0 | 0 | 21 | 0 | 0 | 0 | 0 | 19 | 0 | 0 | 0 | 0 | 26 | 2 | 0 | 0 | 0 |
| Apoptosis of germ cells | 15 | 0 | 0 | 0 | 0 | 21 | 0 | 0 | 0 | 0 | 19 | 0 | 0 | 0 | 0 | 27 | 1 | 0 | 0 | 0 |
| 5 weeks after birth | (4) | | | | | (4) | | | | | (4) | | | | | (4) | | | | |
| Abnormalities | 4 | 0 | 0 | 0 | 0 | 4 | 0 | 0 | 0 | 0 | 4 | 0 | 0 | 0 | 0 | 4 | 0 | 0 | 0 | 0 |
| 10 weeks after birth | (4) | | | | | (4) | | | | | (4) | | | | | (4) | | | | |
| Abnormalities | 4 | 0 | 0 | 0 | 0 | 4 | 0 | 0 | 0 | 0 | 4 | 0 | 0 | 0 | 0 | 4 | 0 | 0 | 0 | 0 |

[a] Vehicle control (corn oil, 5 mL/kg). Figures in parentheses indicate number of fetuses or offspring examined.
– : not observed, ± : very slight, + : slight, ++ : moderate, +++ : severe.

**Table 7.** Morphometric analysis of spermatogenesis of the offspring exposed to 500 mg/kg of di-(2-ethylhexyl)phthalate (DEHP) during gestational days 7-18 5 weeks after birth (Experiment 2).

| | DEHP 0 mg/kg [a] | DEHP 500 mg/kg |
|---|---|---|
| (Number of offspring examined) | (4) | (4) |
| Group 1 (Stage I~VI) | | |
| Count of germ cells in a seminif. tubule | 1098.5 ± 43.4 | 1150.8 ± 110.9 |
| Count of Sertoli cells in a seminif. tubule | 133.8 ± 7.9 | 130.8 ± 4.6 |
| Germ cells/Sertoli cells | 8.2 ± 0.7 | 8.8 ± 1.1 |
| Group 2 (Stage VII~VIII) | | |
| Count of germ cells in a seminif. tubule | 1026.5 ± 84.3 | 1039.3 ± 24.4 |
| Count of Sertoli cells in a seminif. tubule | 137.0 ± 7.4 | 120.5 ± 9.0 |
| Germ cells/Sertoli cells | 7.5 ± 0.9 | 8.7 ± 0.7 |
| Group 3 (Stage IX~XI) | | |
| Count of germ cells in a seminif. tubule | 933.8 ± 66.5 | 938.3 ± 20.9 |
| Count of Sertoli cells in a seminif. tubule | 135.3 ± 3.0 | 125.0 ± 8.2 |
| Germ cells/Sertoli cells | 6.9 ± 0.6 | 7.5 ± 0.4 |
| Group 4 (Stage XII~XIV) | | |
| Count of germ cells in a seminif. tubule | 768.5 ± 28.9 | 738.8 ± 62.9 |
| Count of Sertoli cells in a seminif. tubule | 130.8 ± 7.0 | 127.0 ± 9.7 |
| Germ cells/Sertoli cells | 5.9 ± 0.5 | 5.8 ± 0.2 |

Values represent mean ± S.D.
[a] Vehicle control (corn oil, 5 mL/kg).

butyl)phthalate (DBP). They made oral administration of DBP at doses of 0.5, 5, 50, 100 and 500 mg/kg to pregnant rats from G12 to 21, and observed histopathological changes in fetal testes such as degeneration of seminiferous tubules, focal interstitial cell hyperplasia and adenoma at 500 mg/kg, but not at 100 mg/kg. Parks *et al.* (2000) treated maternal rats with 750 mg/kg of DEHP from G14 to postnatal day 3 and observed the appearance of multinucleated genocytes and hyperplasia of interstitial cells in the testis of G20 fetuses and in offspring at Day 3 of lactation. Thus, the present study has confirmed the characteristics of phthalate toxicity on testicular development in rats, which seems to occur in spite of differences in esterifying alcohol and administration protocol. The no-observed effect-level of DEHP on the testicular development of rats by *in utero* exposure during the period of organogenesis was 125 mg/kg. Target cells of the testicular toxicity of phthalates are the germ cells in the fetal rat, while they are the Sertoli cells in the adult rat when the blood-tes-

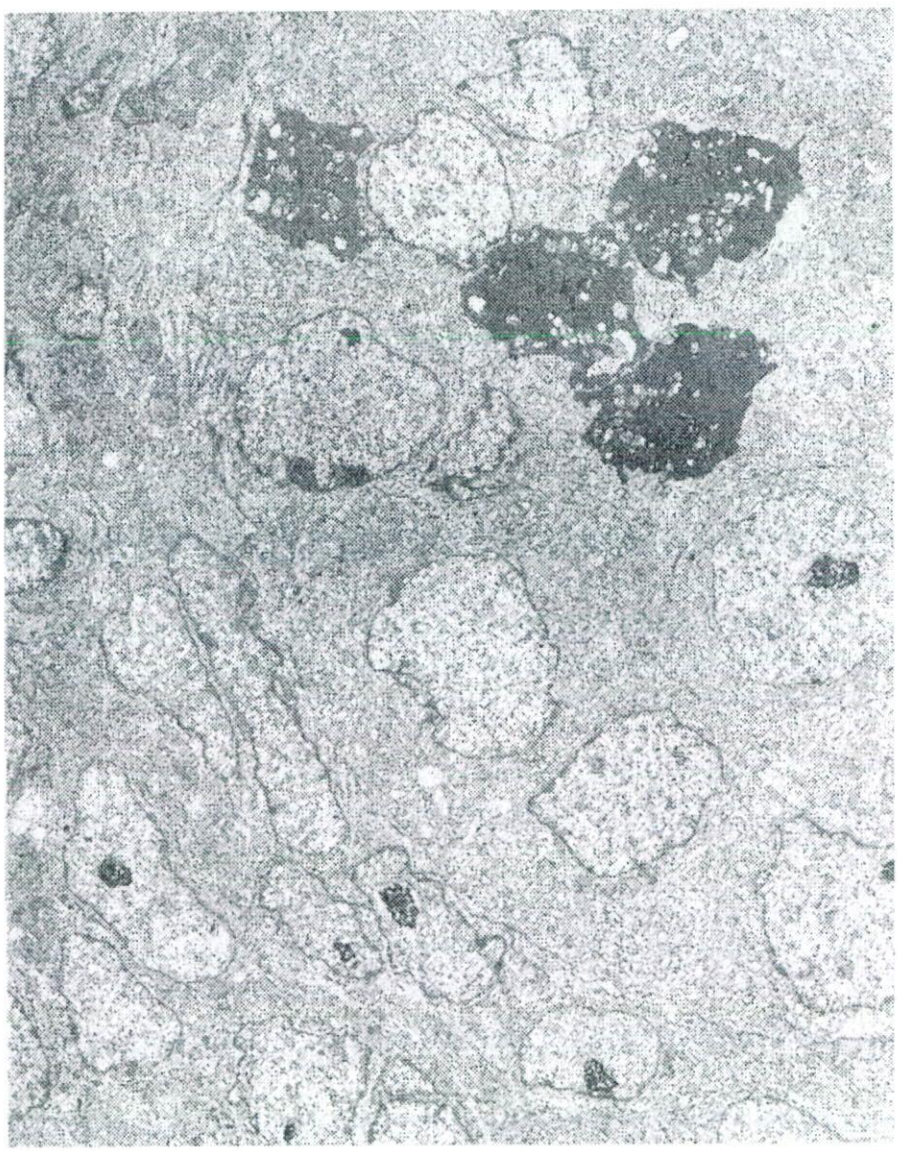

**Photo 7.** An electron micrograph of genital ridge of a rat fetus on gestation day 16 treated with 1000 mg/kg of DEHP, showing degenerated germ cells. ×2830.

tis barrier is established (Creasy *et al.*, 1983, Saitoh *et al.*, 1997, de Kretser and Kerr, 1994).

In the present study, EE was used as a reference compound, considering some interventions of estrogenic activity of DEHP for its toxicity on the testis. The result was negative for this consideration, although some relation may have existed to the increase in embryonic mortality. Estrogenic activity of various phthalate esters was investigated by Zacharewski *et al.* (1998). They observed weak estrogen receptor affinity *in vitro* for some phthalate esters other than DEHP, but no estrogenic activity *in vivo* for any of the phthalate esters by rat uterotropic assay. On the other hand, anti-androgenic activity has been suggested as one of the mechanisms of testicular toxicity of phthalate esters (Mylchreest *et al.*, 1998). Mylchreest *et al.* (1999) observed disturbances in male reproductive development with 500 mg/kg of DBP comparable to 100 mg/

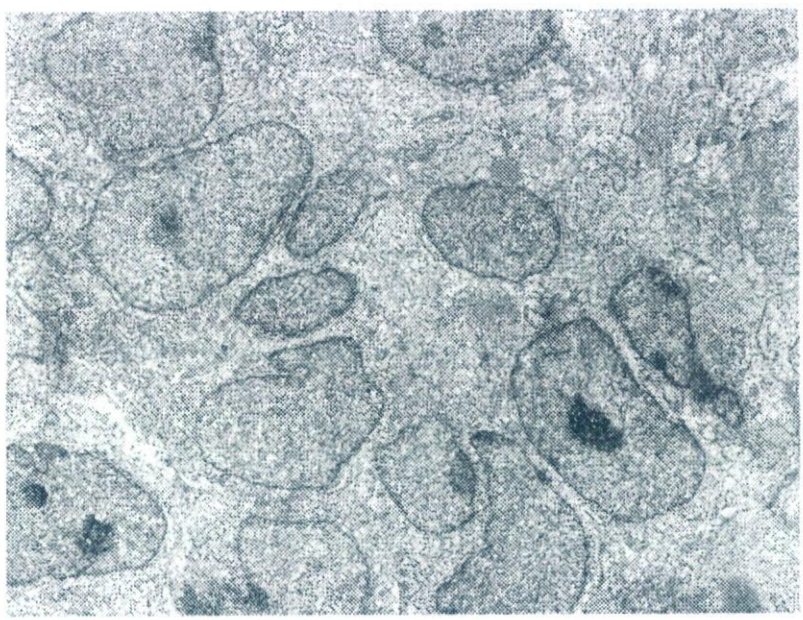

**Photo 8-a.** An electron micrograph of testis of a rat fetus on gestation day 18 treated with 1000 mg/kg of DEHP, showing decreased number of lipid droplets in small-sized interstitial cells. ×3140.

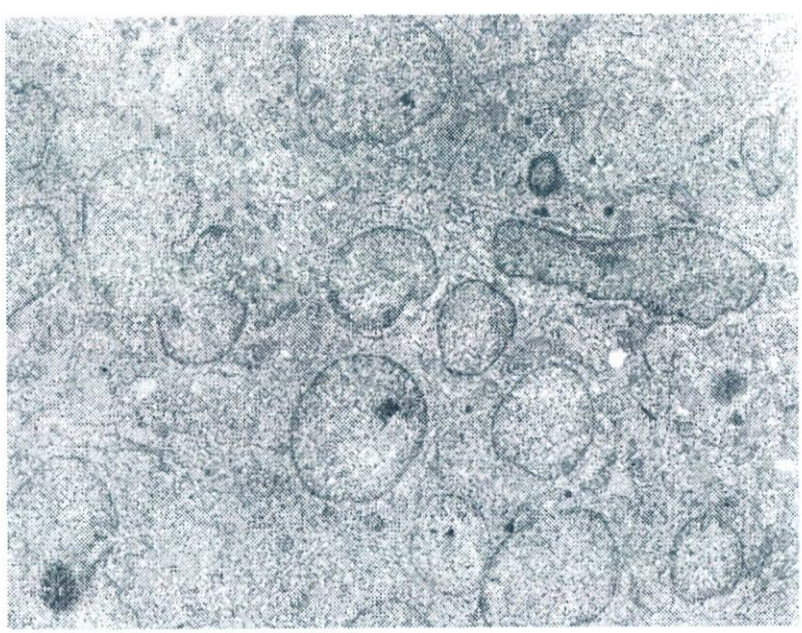

**Photo 8-b.** An electron micrograph of testis of a rat fetus on gestation day 20 treated with 1000 mg/kg of DEHP, showing decreased number of lipid droplets in small-sized interstitial cells. ×3140.

kg of flutamide, a known anti-androgen, but they could not confirm any interaction of phthalate with androgen receptor *in vitro*. They explained that DBP exerted its anti-androgenic activity by indirectly interfering with androgen signaling pathways (Mylchreest and Foster, 2000). Parks *et al.* (2000) observed inhibition of testosterone production of fetal testis (G17-20) with DEHP (750 mg/kg) in the experiment cited above. In the present study, increase of androgen receptor-positive interstitial cells was observed in G20 fetal testis in the groups treated with DEHP at 250 mg/kg and above. It is conceivable that interstitial cells and androgen receptors are increased by compensatory responses to reduced testosterone levels. Thus, anti-androgenic activity of DEHP is suggested from the observation of the present study, although malformations of male genital organs typical of anti-androgens such as flutamide (Mylchreest *et al.*, 1998, 1999) were not observed with DEHP up to 1000 mg/kg in the present study.

The present study has demonstrated that testicular damage in fetal rats produced by DEHP at 500 mg/kg (but not at 1000 mg/kg) had been repaired by 7 weeks of age. This was confirmed in the second experiment at 5 and 10 weeks of age. Expression of androgen receptors in testicular cells was normal in these stages of rats. Moreover, examination of sperm in off-

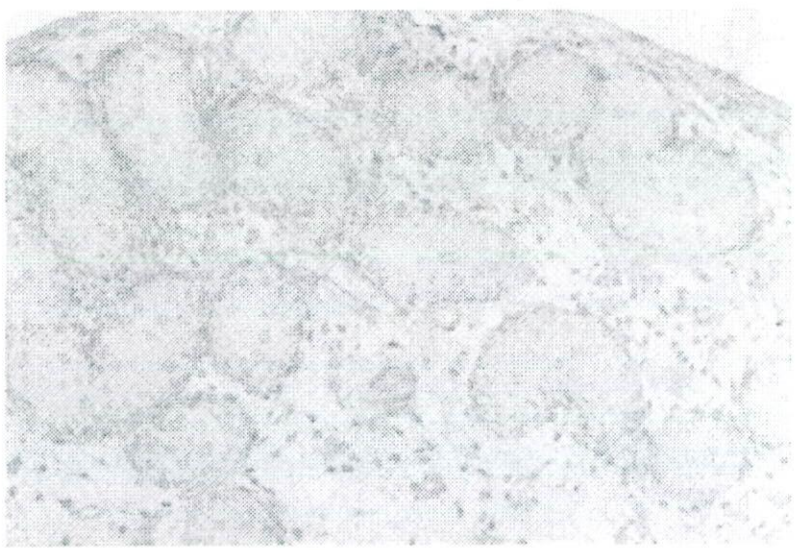

**Photo 9-a.** Immunohistochemical staining of androgen receptors in testis on rat fetus on G20 from the control group. Positive signals are observed on peritubular myoid cells and interstitial cells. ×175.

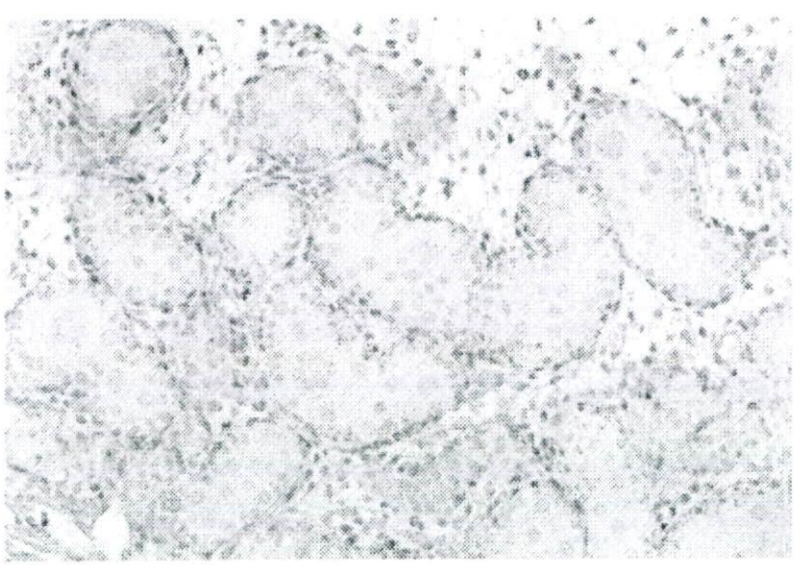

**Photo 9-b.** Immunohistochemical staining of androgen receptors in testis of rat fetus on G20 from the group treated with 500 mg/kg of DEHP. Interstitial cells with positive androgen-receptor signals are increased. ×175.

spring of DEHP-treated rats at 10 weeks of age showed no abnormal features of sperm function and morphology.

## REFERENCES

Calley, D., Autian, J. and Guess, W.L. (1966): Toxicology of a series of phthalate esters. J. Pharm. Sci., **55**, 158-162.

Cater, B.R., Cook, M.W., Gangolli, S.D. and Grasso, P. (1977): Studies on dibutyl phthalate-induced testicular atrophy in the rat: effect on zinc metabolism. Toxicol. Appl. Pharmacol., **41**, 609-618.

Creasy, D.M., Beech, L.M., Gray, T.J.B. and Butler, W.H. (1987): The ultrastructural effect of di-*n*-pentyl phthalate on the testis of the mature rats. Exp. Mol. Pathol., **46**, 357-371.

Creasy, D.M., Foster, J.R. and Foster, P.M.D. (1983): The morphological development of di-*n*-pentyl phthalate induced testicular atrophy in the rat. J. Pathol., **139**, 309-321.

Dalgaard, M., Nellemann, C., Lam, H.R., Sorensen, I.K. and Ladefoged, O. (2001): The acute effects of mono(2-ethylhexyl)phthalate (MEHP) on testes of prepubertal Wistar rats. Toxicol. Lett., **122**, 69-79.

de Kretser, D.M. and Kerr, J.B. (1994): The cytology of the testis. In "Physiology of Reproduction", 2nd ed., (Knobil, E. and Neill, J.D., eds.), pp. 1177-1290, Raven Press, New York.

Dym, M. and Clermont, Y. (1970) Role of spermatogonia in the repair of the seminiferous epithelium following x-irradiation of the rat testis. Am. J. Anat., **128**, 265-282.

Gangolli, S.D. (1982): Testicular effects of phthalate esters. Environ. Health Perspect., 45, 77-84.

Gray, T.J. and Butterworth, K.R. (1980): Testicular atrophy produced by phthalate esters. Arch. Toxicol. Suppl., **4**, 452-455.

**Table 8.** Examination of epididymal spermatozoa at 10 weeks after birth in the offspring exposed to di-(2-ethylhexyl) phthalate (DEHP) during gestational days 7-18 (Experiment 2).

| | DEHP (mg/kg) | | | |
|---|---|---|---|---|
| | 0 [a] | 125 | 250 | 500 |
| Animals examined | 4 | 4 | 4 | 4 |
| Sperm counts (per cauda epididymis) [b] | 176.7 ± 55.7 | 142.9 ± 51.2 | 149.9 ± 48.9 | 175.0 ± 49.8 |
| Sperm counts/cauda epididymis weight (g) [b] | 1015.2 ± 241.0 | 878.0 ± 305.6 | 872.9 ± 198.7 | 992.1 ± 335.2 |
| Sperm motility | | | | |
| Rate of motile sperm (%) [b] | 98.1 ± 1.2 | 96.6 ± 1.0 | 98.4 ± 1.1 | 97.2 ± 1.8 |
| Rate of progressive sperm (%) [b] | 84.4 ± 5.2 | 85.5 ± 1.8 | 88.7 ± 2.0 | 88.4 ± 3.2 |
| Sperm morphology | | | | |
| Sperms examined | 800 | 800 | 800 | 800 |
| Sperms with abnormalities | 34 | 49 | 45 | 44 |
| Abnormality rate (%) [b] | 4.3 ± 1.7 | 6.1 ± 1.7 | 5.6 ± 5.5 | 5.5 ± 1.8 |
| Types and incidence (%) of abnormal sperms | | | | |
| Pin head | 0 | 0 | 0.3 | 0.3 |
| Amorphous head | 0 | 0 | 0.1 | 0 |
| Short head | 0.1 | 0 | 0 | 0.1 |
| Banana head | 0 | 0.1 | 0 | 0 |
| Reduced hock | 0.1 | 0.5 | 0.4 | 0.3 |
| No hock | 0 | 0.1 | 0.1 | 0.1 |
| Excessive hock | 0 | 0 | 0.1 | 0 |
| Bent flagellum | 0.1 | 0.1 | 0 | 0 |
| Broken flagellum | 0.1 | 0.5 | 0.1 | 0.4 |
| Bent neck | 0.4 | 0.6 | 0.1 | 0.6 |
| Isolated head | 3.3 | 4.1 | 4.4 | 3.8 |
| Two heads, one tail | 0.1 | 0 | 0 | 0 |

[a] Vehicle control (corn oil, 5 mL/kg). [b] Values represent mean ± S.D.

Gray, T.J., Butterworth, K.R., Gaunt, I.F., Grasso, G.P. and Gangolli, S.D. (1977): Short-term toxicity study of di-(2-ethylhexyl) phthalate in rats. Food Cosmet. Toxicol., **15**, 389-399.

Gray, T.J. and Gangolli, S.D. (1986): Aspects of the testicular toxicity of phthalate esters. Environ. Health Perspect., **65**, 229-235.

Matsui, H., Toyoda, K., Kawanishi, T., Mitsumori, K. and Takahashi, M. (1996): Direct toxic effects of ethylene-1,2-dimethanesulfonate(EDS) on the rat epididymis. J. Toxicol. Pathol., **9**, 65-72.

Mylchreest, E., Cattley, R.C. and Foster, P.M.D. (1998): Male reproductive tract malformations in rats following gestational and lactational exposure to di(*n*-butyl) phthalate: An antiandrogenic mechanism? Toxicol. Sci., **43**, 47-60.

Mylchreest, E. and Foster, P.M.D. (2000): DBP exerts its antiandrogenic activity by indirectly interfering with androgen signaling pathways. Toxicol. Appl. Pharmacol., **168**, 174-175.

Mylchreest, E., Sar, M., Cattley, R.C. and Foster, P.M.D. (1999): Disruption of androgen-regulated male reproductive development by di(*n*-butyl) phthalate during late gestation in rats is different from flutamide. Toxicol. Appl. Pharmacol., **156**, 81-95.

Mylchreest, E., Wallace, D.G., Cattley, R.C. and Foster, P.M.D. (2000): Dose-dependent alterations in androgen-regulated male reproductive development in rats exposed to di-(*n*-butyl) phthalate during late gestation. Toxicol. Sci., **55**, 143-151.

Ono, H., Saito, Y., Imai, K. and Kato, M. (2004): Subcellular distribution of di-(2-ethylhexyl) phthalate in rat testis. J. Toxicol. Sci., **29**, 113-124.

Parks, L.G., Ostby, J.S., Lambright, C.R., Abbott, B.D., Klinefelter, G.R., Barlow, N.J. and Gray, L.E.Jr. (2000): The plasticizer diethylhexyl phthalate induces malformation by decreasing fetal testosterone synthesis during sexual differentiation in the male rat. Toxicol. Sci., **58**, 339-349.

Saitoh, Y., Usumi, K., Nagata, T., Marumo, H., Imai, K. and Katoh, M. (1997): Early changes in the rat testes induced by di-(2-ethylhexyl) phthalate and 2,5-hexandione – Ultrastructure and lanthanum trace study. J. Toxicol. Pathol., **10**, 51-57.

Sato, M., Ohta, R., Kojima, K. and Shirota, M. (2002a): Strain differences in the spontaneous incidence of sperm morphological abnormalities in Hatano rats. J. Vet. Med. Sci., **64**, 389-390.

Sato, M., Ohta, R., Kojima, K., Shirota, M., Koibuchi, H., Asai, S., Watanabe, G. and Taya, K. (2002b): A comparative study of puberty, and plasma gonadotropin and testicular hormone levels in two inbred strains of Hatano rats. J. Reprod. Dev., **48**, 111-119.

Sato, M., Ohta, R., Wada, K., Marumo, H., Shirota, M. and Nagao, T. (2000): Utilization of a computer-assisted sperm motion analysis system to examine effects of dinoseb on rat sperm. J. Reprod. Dev., **46**, 279-286.

Yasuda, M., Kihara, T. and Tanimura, T. (1985): Effect of ethynyl estradiol on the differentiation of mouse fetal testis. Teratology, **32**, 113-118.

Yoshimura, I. (1986): Statistical Analysis of Toxicological and Pharmacological Data. (in Japanese) Scientists (Publisher), Tokyo.

Zacharewski, T.R., Meek, M.D., Clemons, J.H., Wu, Z.F., Fielden, M.R. and Mattews, J.B. (1998): Examination of the *in vivo* estrogenic activities of eight commercial phthalate esters. Toxicol. Sci., **46**, 282-293.

Cell

# Estrogen Prevents Bone Loss via Estrogen Receptor α and Induction of Fas Ligand in Osteoclasts

Takashi Nakamura,[1,2,9] Yuuki Imai,[1,3,9] Takahiro Matsumoto,[1,2] Shingo Sato,[4] Kazusane Takeuchi,[1] Katsuhide Igarashi,[5] Yoshifumi Harada,[6] Yoshiaki Azuma,[6] Andree Krust,[7] Yoko Yamamoto,[1] Hiroshi Nishina,[4] Shu Takeda,[4] Hiroshi Takayanagi,[4] Daniel Metzger,[7] Jun Kanno,[5] Kunio Takaoka,[3] T. John Martin,[8] Pierre Chambon,[7] and Shigeaki Kato[1,2,*]

[1]Institute of Molecular and Cellular Biosciences, University of Tokyo, Yayoi 1-1-1, Bunkyo-ku, Tokyo 113-0032, Japan

[2]Exploratory Research for Advanced Technology, Japan Science and Technology Agency, Honcho 4-1-8, Kawaguchi, Saitama 332-0012, Japan

[3]Department of Orthopaedic Surgery, Osaka City University Graduate School of Medicine, Asahimachi 1-4-3, Abeno-ku, Osaka, 545-8585, Japan

[4]Tokyo Medical and Dental University, Yushima 1-5-45, Bunkyo-ku, Tokyo 113-8510, Japan

[5]Division of Cellular and Molecular Toxicology, National Institute of Health Sciences, 1-18-1 Kamiyoga, Setagaya-ku, Tokyo 158-8501, Japan

[6]Teijin Institute for Biomedical Research, Asahigaoka 4-3-2, Hino, Tokyo 191-8512, Japan

[7]Institut de Génétique et de Biologie Moleculaire et Cellulaire, Departement of Physiological Genetics / Inserm, U-596 / CNRS, UMR7104 / Université Louis Pasteur, Illkirch, Strasbourg, F-67400 France

[8]St. Vincent's Institute of Medical Research, 9 Princes Street, Fitzroy VIC 3065, Australia

[9]These authors contributed equally to this work.

*Correspondence: uskato@mail.ecc.u-tokyo.ac.jp

DOI 10.1016/j.cell.2007.07.025

## SUMMARY

Estrogen prevents osteoporotic bone loss by attenuating bone resorption; however, the molecular basis for this is unknown. Here, we report a critical role for the osteoclastic estrogen receptor α (ERα) in mediating estrogen-dependent bone maintenance in female mice. We selectively ablated ERα in differentiated osteoclasts ($ER\alpha^{\Delta Oc/\Delta Oc}$) and found that $ER\alpha^{\Delta Oc/\Delta Oc}$ females, but not males, exhibited trabecular bone loss, similar to the osteoporotic bone phenotype in postmenopausal women. Further, we show that estrogen induced apoptosis and upregulation of Fas ligand (FasL) expression in osteoclasts of the trabecular bones of WT but not $ER\alpha^{\Delta Oc/\Delta Oc}$ mice. The expression of ERα was also required for the induction of apoptosis by tamoxifen and estrogen in cultured osteoclasts. Our results support a model in which estrogen regulates the life span of mature osteoclasts via the induction of the Fas/FasL system, thereby providing an explanation for the osteoprotective function of estrogen as well as SERMs.

## INTRODUCTION

Bone remodeling is a dynamic metabolic process. The destruction or "resorption" of pre-existing bone by mature osteoclasts is followed by the formation of new bone by osteoblasts. Osteoblasts are derived from pleiotropic mesenchymal stem cells in the bone marrow. Mature osteoclasts are multinuclear, macrophage-like cells, derived from hematopoietic stem cells also in the bone marrow. Bone resorption and deposition are tightly coupled, and their balance defines both bone mass as well as quality. The regulation of bone remodeling is complex. A number of systemic hormones and transcription factors directly regulate the proliferation and differentiation of osteoblasts and osteoclasts (Karsenty, 2006; Karsenty and Wagner, 2002; Rodan and Martin, 2000; Teitelbaum and Ross, 2003). Additionally, the indirect cellular communication among groups of bone cells is also physiologically critical for bone growth and remodeling (Martin and Sims, 2005; Mundy and Elefteriou, 2006). The molecular and genetic mechanisms governing bone cell fate have been intensively studied; however, how the life span of bone cells is determined on a molecular level remains elusive.

Estrogen is a key hormone in bone remodeling in several species. The osteoprotective action of estrogen is demonstrable in rodents and is clinically important in humans, particularly older women (Chien and Karsenty, 2005;

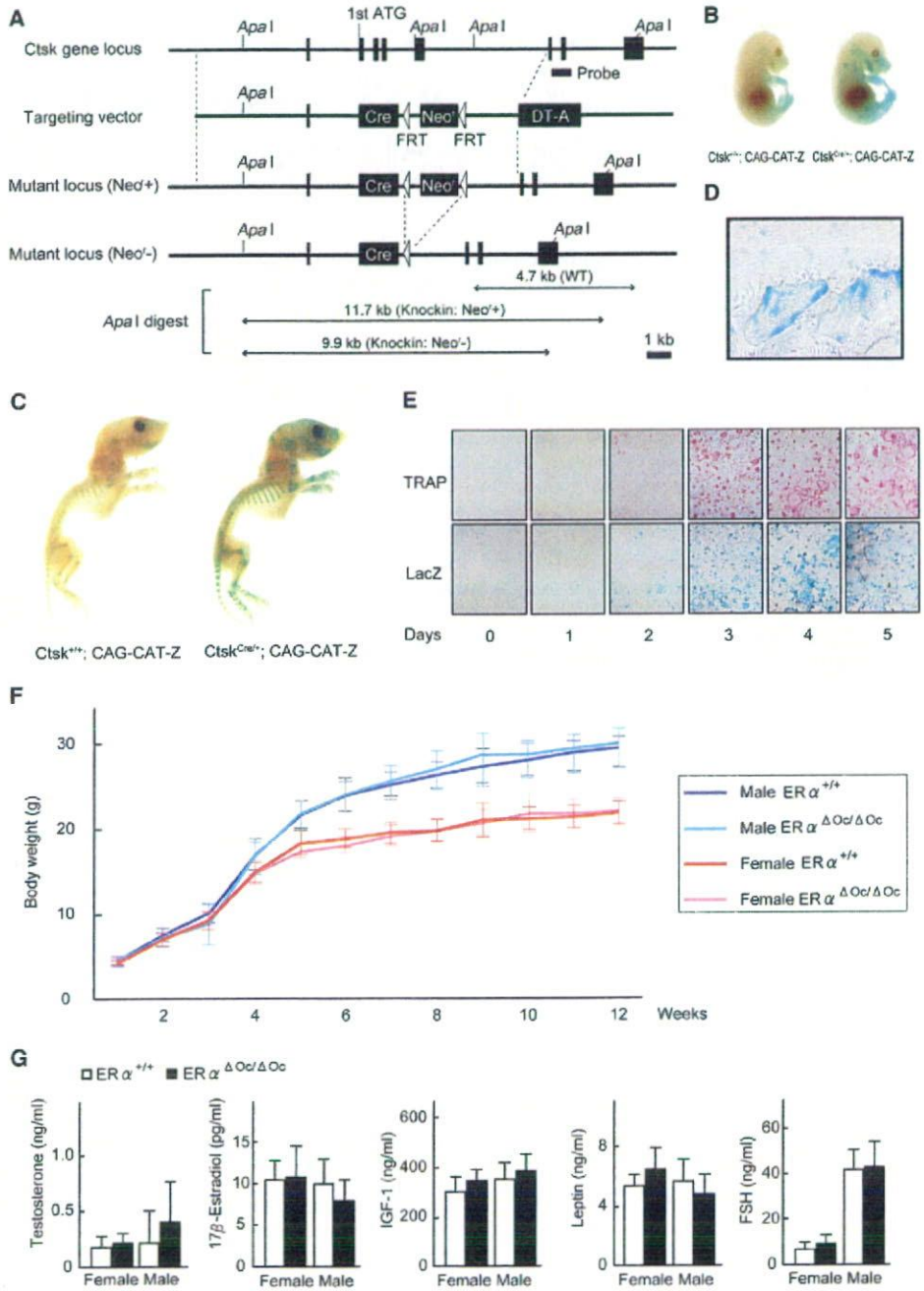


**Figure 1. Generation of Knockin Mice Selectively Expressing Cre in Mature Osteoclasts**

(A) Illustration of the targeting strategy for insertion of the *Cre* gene into the mouse *Cathepsin K* (*Ctsk*) gene. A targeting vector was generated to contain the *Cre* cDNA at the endogenous ATG start site, followed by a *FRT* (Flp-recombinase target)-flanked *Neo*$^r$ cassette. The *DT-A* (diphtheria toxin-A) gene was also inserted to avoid random integrations.

(B and C) *Ctsk-Cre* mice were then crossed with *CAG-CAT-Z* mice. β-galactosidase activity derived from the activated *LacZ* reporter gene was monitored to test if expressed Cre excised the *loxP* sites in mature osteoclasts. LacZ expression patterns reflected the localization patterns of mature osteoclasts in the developing bone at 16.5 days post coitum embryos and in the skeletal tissues of 7-day-old pups.

(D) The LacZ expression induced by Cre-mediated excision was also seen in osteoclasts attached to trabecular bone in the lumber vertebrae of 12-week-old mice.

(E) LacZ expression was induced during osteoclastogenesis. Osteoclast-like cells that differentiated from bone-marrow macrophages following culture in the presence of M-CSF and RANKL were stained with TRAP (tartrate-resistant acid phosphatase), a mature osteoclast marker.

Delmas, 2002; Raisz, 2005; Rodan and Martin, 2000). Estrogen deficiency in postmenopausal women frequently leads to osteoporosis, the most common skeletal disorder. Similarly, ovariectomy clearly produces an osteoporotic bone phenotype in mice. Osteoporotic bone loss is the result of high bone turnover in which bone resorption outpaces bone deposition (Rodan and Martin, 2000; Teitelbaum, 2007). This imbalance in bone turnover that is induced by estrogen deficiency in women and female rodents can be ameliorated with bio-available estrogens including selective estrogen receptor modulators (SERMs) (Riggs and Hartmann, 2003).

Estrogen and SERMs primarily act by regulating gene transcription via estrogen receptors (ERα, ERβ) (Couse and Korach, 1999; Shang and Brown, 2002). ERs belong to the nuclear receptor gene superfamily and act as ligand-inducible transcriptional factors (Mangelsdorf et al., 1995). ER dimers directly or indirectly associate with specific DNA elements in the target gene promoter (Shang and Brown, 2002) and control transcription through reorganizing chromatin structure and histone modifications (Belandia and Parker, 2003). Genetic mouse models (KO mice) lacking ERα (*ERα*$^{-/-}$) and ERβ (*ERβ*$^{-/-}$) provide insights into ER function (Mueller and Korach, 2001; Windahl et al., 2002). In mice, though ERα appears to be the major receptor in most estrogen target tissues including bone (Sims et al., 2003), neither clear bone loss nor high bone turnover is detectable in ERα single or ERα/ERβ double-KO females (Syed and Khosla, 2005; Windahl et al., 2002). This unexpected maintenance of bone mass in female mutants is presumed to be due to unphysiologically elevated levels of other osteoprotective hormones, like androgens. Systemic defects in the hypothalamus caused by ER inactivation appear to impair the negative feedback system of hormone production (Syed and Khosla, 2005). This leads to an excess in estrogen precursors, notably androgens. In fact, the anabolic effects of androgens mediated by the androgen receptor (AR) are evident in female mice (Kawano et al., 2003; Sims et al., 2003). In males, estrogen is also osteoprotective, as is evident by the development of osteopenia in male patients genetically deficient in ERα (Smith et al., 1994) or aromatase activity (Simpson and Davis, 2001). Thus, irrespective of the accumulating clinical and basic research data on the osteoprotective actions of estrogen and SERMs, the molecular basis of this osteoprotection in females remains elusive.

To study the molecular interactions behind the antibone resorptive actions of estrogen in women and female animals, we genetically ablated ERα in mature osteoclasts (*ERα*$^{\Delta Oc/\Delta Oc}$). Selective ablation of ERα in differentiated osteoclasts (*ERα*$^{\Delta Oc/\Delta Oc}$) was accomplished by crossing a *Cathepsin K-Cre* knockin mouse with a floxed *ERα* mouse. This resulted in clear trabecular bone loss and high bone turnover associated with increased osteoclast numbers in females but not in males. In the female mutants, further bone loss following ovariectomy was not significant and recovery by estrogen was ineffective in the trabecular areas of long bones and lumbar vertebral bodies. Upregulated expression of *Fas ligand* (*FasL*) gene, and increased apoptosis in differentiated osteoclasts by estrogen was found in the intact bone of wild-type females but undetectable in *ERα*$^{\Delta Oc/\Delta Oc}$ females. Induction of FasL and apoptosis by estrogen as well as a SERM also required ERα in cultured osteoclasts. Thus, we propose that the osteoprotective actions of estrogen and SERMs are mediated at least in part through osteoclastic ERα in trabecular bone, and the life span of mature osteoclasts is regulated through the activation of the FasL signaling.

## RESULTS

### Generation of Osteoclast-Specific *ERα* Gene Disruption by Knocked-In *Cre* in the *Cathepsin K* Gene

To specifically disrupt *ERα* gene in mature osteoclasts, we knocked in *Cre* into the gene locus of *Cathepsin K* (*Ctsk*$^{Cre/+}$) (Figures 1A, S1A, and S1B), a gene known to be expressed in differentiated osteoclastic cells arising from hematopoietic stem cells. This gene is functionally indispensable for mature osteoclasts (Saftig et al., 1998). Only one copy appears enough to support normal bone formation and bone turnover, since heterozygous mutant mice of *Cathepsin K* (*Ctsk*$^{+/-}$) have no obvious bone phenotype (Gowen et al., 1999; Li et al., 2006; Saftig et al., 1998) . Clear, bone-specific expression of the *Cre* transcript in the adult *Ctsk*$^{Cre/+}$ mice was observed in the tested tissues (Figure S1C). To confirm Cre protein expression, the *Ctsk*$^{Cre/+}$ mice were crossed with tester mice (*CAG-CAT-Z*). These mice were genetically engineered to express β-galactosidase by excision of the transcribed stop sequence in front of the *β-galactosidase* gene (*LacZ*) in cells expressing Cre (Sakai and Miyazaki, 1997). β-galactosidase expression visualized by LacZ staining was observed in the bones of 16.5 dpc embryos and 7-day-old pups of *Ctsk*$^{Cre/+}$; *CAG-CAT-Z* mice. Expression patterns were consistent with the appearance and skeletal localization of functionally mature osteoclasts (Figures 1B and 1C). Histochemical staining of LacZ in the lumbar vertebrae of 12-week-old mice was localized in multinuclear osteoclasts (Figure 1D) but not seen in osteoblasts and osteocytes (Figure S1D) and the hypothalamus (Figure S1E). Since *Cathepsin K* gene expression is evident in differentiated osteoclasts (Saftig et al., 1998), we used an in vitro culture cell system to test whether Cre expression was driven by the endogenous promoter that is induced at the time of osteoclast differentiation. Osteoclast-precursor cells derived from bone marrow

(F) The growth curve of *ERα*$^{\Delta Oc/\Delta Oc}$ mice was indistinguishable from that of the control mice. Data are represented as mean ± SEM.
(G) Serum hormone levels were normal in 12-week-old *ERα*$^{\Delta Oc/\Delta Oc}$ (filled column) versus *ERα*$^{+/+}$ (open column) mice (n = 10–11 animals per genotype). Data are represented as mean ± SEM.

were cytodifferentiated for 1 week in the presence of M-CSF (macrophage colony stimulating factor) and RANKL (receptor activator of NFκB ligand) (Koga et al., 2004). TRAP-positive osteoclasts emerged after 3 days of culture (Figure 1E). The number of TRAP-positive osteoclasts and the number of LacZ-expressing cells simultaneously increased. In the contrast, the LacZ expression was not detected in primary cultured osteoblasts derived from the calvaria (Figure S1F). In view of both our in vivo and in vitro observations, we conclude that the $Ctsk^{Cre/+}$ mouse line expresses Cre in differentiated osteoclasts. Moreover, estrogen response in bone mass control was not distinguishable in between $Ctsk^{Cre/+}$ and $Ctsk^{+/+}$ mice (Figure S2A).

We then crossed floxed *ERα* mice (Dupont et al., 2000) with $Ctsk^{Cre/+}$ mice to disrupt ERα in differentiated osteoclasts ($ER\alpha^{\Delta Oc/\Delta Oc}$). Excision of the *ERα* gene (Figure S1G) was confirmed by Southern blotting of DNA from adult female and male (data not shown) bone as well as in cultured mature osteoclasts (Figure S1H). No overt differences were observed in the growth curve, reproduction, or tissues for up to 12 weeks of age (Figure 1F) between the $Ctsk^{Cre/+}$; $ER\alpha^{+/+}$ ($ER\alpha^{+/+}$) and the $Ctsk^{Cre/+}$; $ER\alpha^{flox/flox}$ ($ER\alpha^{\Delta Oc/\Delta Oc}$) mice, with the exception of the female bones. Serum levels of sex hormones and bone remodeling regulators such as IGF-I, leptin, and follicle-stimulating hormone (Sun et al., 2006; Takeda et al., 2002) appeared unchanged in both male and female $ER\alpha^{\Delta Oc/\Delta Oc}$ mice at 12 weeks (Figure 1G).

## Osteopenia Occurred in Osteoclast-Specific ERα KO Females But Not Males

The 12-week-old $ER\alpha^{\Delta Oc/\Delta Oc}$ females exhibited a clear reduction in bone mineral density (BMD) in the femurs (Figures 2A–2C) and tibiae (data not shown) when compared with $ER\alpha^{+/+}$ mice. Though cortical bone appeared unaffected, trabecular bone loss (Figure 2A) with significant reduction of trabecular bone volume (BV/TV) (Figure 2F) was clearly seen. This is similar to the osteoporotic abnormalities observed in women during natural menopause or following ovariectomy (Delmas, 2002; Tolar et al., 2004). However, unlike men deficient in aromatase or ERα activity (Simpson and Davis, 2001; Smith et al., 1994), $ER\alpha^{\Delta Oc/\Delta Oc}$ males unexpectedly exhibited no clear bone loss even in the trabecular areas (Figures 2A–2C). In $ER\alpha^{\Delta Oc/\Delta Oc}$ females, both the bone-formation rate, estimated by double-calcein labeling (Figure 2D), as well as the bone-resorption rate, estimated from TRAP-positive differentiated osteoclast numbers (Figure 2E), were increased, indicating high bone turnover. Histomorphometric analyses of $ER\alpha^{\Delta Oc/\Delta Oc}$ females supported the observation of accelerated bone resorption, as increased numbers of osteoclasts (Oc. S/BS and N. Oc/BS) were observed together with more eroded bone surface (ES/BS in Figure 2F). Bone formation was also enhanced as the rates of mineral apposition (MAR) and bone formation (BFR/BS) were both upregulated without an increase in osteoblast numbers (Ob.S/BS) (Figure 2F). Thus, considering all of these findings, it is conceivable that the increased number of differentiated osteoclasts following ERα ablation accelerates bone resorption over formation, leading to bone loss in the trabecular areas.

## No Further Bone Loss Results from Estrogen Deficiency in $ER\alpha^{\Delta Oc/\Delta Oc}$ Females

To verify whether osteoclastic ERα indeed mediates osteoprotective estrogen actions, estrogen action was investigated by ovariectomy (OVX) of 12-week-old female mice. As expected, OVX in $ER\alpha^{+/+}$ females resulted in significantly reduced BMD particularly in the trabecular bone (Figures 3A and 3B) but not in the cortical bone (Figure 3C). Consistent with previous reports, (Kimble et al., 1995; Teitelbaum and Ross, 2003), estrogen deficiency following OVX upregulated the serum levels of cytokines like TNFα and IL-1α (Figure 3D). These cytokines enhance bone resorption through stimulation of osteoclastogenesis, leading to the loss of bone mass (Teitelbaum and Ross, 2003). OVX did not further reduce BMD or trabecular bone volume of the femurs of $ER\alpha^{\Delta Oc/\Delta Oc}$ females (Figure 3B) nor affect increased number of TRAP-positive osteoclasts (see lower panel in Figure 3A) despite upregulation of serum cytokines. This suggests that the expression of cytokines known to regulate bone resorption is not under the control of osteoclastic ERα.

## Estrogen Treatment Failed to Rescue the Osteoporotic Bone Phenotype of $ER\alpha^{\Delta Oc/\Delta Oc}$ Mice

Estrogen treatment by estrogen pellet implantation (OVX + E2) for 2 weeks after OVX in $ER\alpha^{+/+}$ mice elicited a dramatic increase in bone mass in both the trabecular and cortical areas of the femurs (data not shown) and lumbar vertebral bodies (Figure 4A). Estrogen action during E2 treatment in female mutants ($ER\alpha^{\Delta Oc/\Delta Oc}$) was not as pronounced as in the $ER\alpha^{+/+}$ females (Figures 4A and 4B), and the increase in the trabecular portions of the distal femurs was slight (data not shown). Histomorphometric analysis of the lumbar vertebral bodies (Figure 4B) supported the idea that E2 treatment in the female mutants was not sufficient to suppress accelerated bone resorption. These in vivo findings in the $ER\alpha^{\Delta Oc/\Delta Oc}$ females suggest that in at least the trabecular areas of the long bones and lumbar vertebral bodies, the osteoprotective estrogen action is primarily mediated via osteoclastic ERα inhibiting bone resorption.

To further test this hypothesis, we investigated ERα protein expression in mature osteoclasts from trabecular bone. Few reports document osteoclastic expression of ERα protein and an estrogen response in both intact animals and in in vitro cultured osteoclasts (Bland, 2000). We therefore reasoned that ER expression ceases during differentiation into mature cells from primary cultures of osteoclast precursors, similar to that observed in other primary culture cell systems such as avian oviduct cells, in which ERα protein expression is drastically decreased during culture (Kato et al., 1989). Using highly sensitive immunohistochemistry, we investigated whether

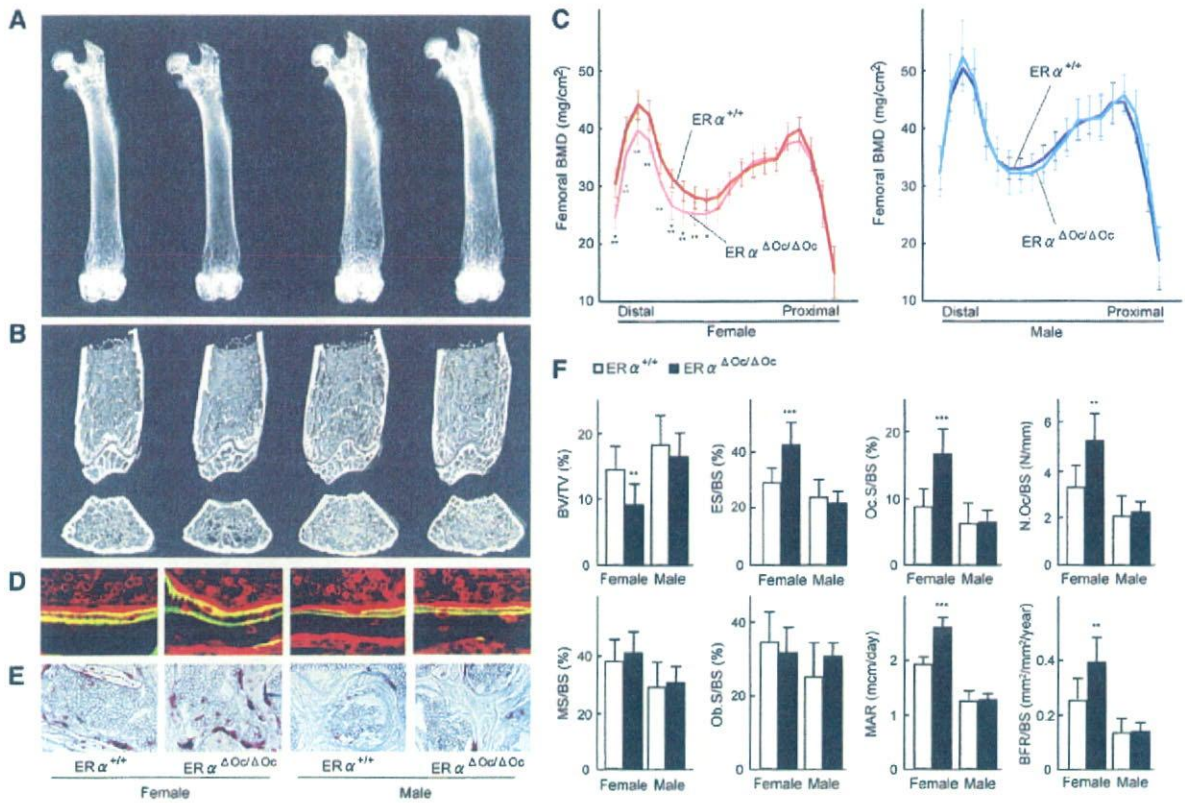


**Figure 2. High Bone Turnover Osteopenia Was Observed in $ER\alpha^{\Delta Oc/\Delta Oc}$ Females But Not Males**

(A) Soft X-ray images of femurs from 12-week-old $Ctsk^{Cre/+}$; $ER\alpha^{flox/flox}$ ($ER\alpha^{\Delta Oc/\Delta Oc}$) mice.

(B) Three-dimensional computed tomography images of the distal femurs and axial sections of distal metaphysis from representative 12-week-old $Ctsk^{Cre/+}$; $ER\alpha^{+/+}$ ($ER\alpha^{+/+}$) and $ER\alpha^{\Delta Oc/\Delta Oc}$ mice.

(C) BMD of each of 20 equal longitudinal divisions of femurs from 12-week-old $ER\alpha^{+/+}$ and $ER\alpha^{\Delta Oc/\Delta Oc}$ mice. (n = 10–11 animals per genotype; Student's t test, $^*p < 0.05$; $^{**}p < 0.01$; $^{***}p < 0.001$). Data are represented as mean ± SEM.

(D) Bone formation was also accelerated in $ER\alpha^{\Delta Oc/\Delta Oc}$ females when two calcein-labeled mineralized fronts visualized by fluorescent micrography were measured in the proximal tibia of 12-week-old mice.

(E) The number of TRAP-positive osteoclasts in the lumbar spine of female mice was increased by selective disruption of ERα in osteoclasts, indicating enhanced bone resorption.

(F) Bone turnover parameters as measured by dynamic bone histomorphometry after calcein labeling indicated high bone turnover in $ER\alpha^{\Delta Oc/\Delta Oc}$ females. Parameters are measured in the proximal tibia of 12-week-old $ER\alpha^{+/+}$ (open column) and $ER\alpha^{\Delta Oc/\Delta Oc}$ (filled column) mice. BV/TV: bone volume per tissue volume. ES/BS: eroded surface per bone surface. Oc.S/BS: osteoclast surface per bone surface. N.Oc/BS: osteoclast number per bone surface. MS/BS: mineralizing surface per bone surface. Ob.S/BS: osteoblast surface per bone surface. MAR: mineral apposition rate. BFR/BS: bone formation rate per bone surface (n = 10–11 animals per genotype; Student's t test, $^*p < 0.05$; $^{**}p < 0.01$; $^{***}p < 0.001$). Data are represented as mean ± SEM.

ERα protein expresses in differentiated osteoclasts in the bone tissues of femur sections from 12-week-old mice. ERα protein expression appeared abundant in osteoblasts and osteocytes of femur sections (Figure 4C) as well as hypothalamus (Figure S2B) from 12-week-old mice, in agreement with a previous report (Zaman et al., 2006). Likewise, expression levels of ERα in primary cultured osteoblasts derived from calvaria of $ER\alpha^{\Delta Oc/\Delta Oc}$ females appeared unaffected (Figure S2C). In contrast, in differentiated osteoclasts of the same femur sections, ERα expression was definitely detectable but very low in the $ER\alpha^{+/+}$ but undetectable in $ER\alpha^{\Delta Oc/\Delta Oc}$ females (Figure 4C).

### Signaling by Osteoclastogenic Factors and Osteoclastogenesis Is Intact in Osteoclasts Deficient in ERα

It is possible that the osteoprotective function of osteoclastic ERα inhibits osteoclastogenesis. To address this issue, osteoclastogenesis was tested in cultured osteoclasts derived from bone-marrow cells of $ER\alpha^{\Delta Oc/\Delta Oc}$ mutants. In this cell culture system, a possible contribution of contaminated immune cells and stromal cells could be excluded, since osteoclastogenesis is only inducible by M-CSF treatment followed by M-CSF + RANKL (Koga et al., 2004).

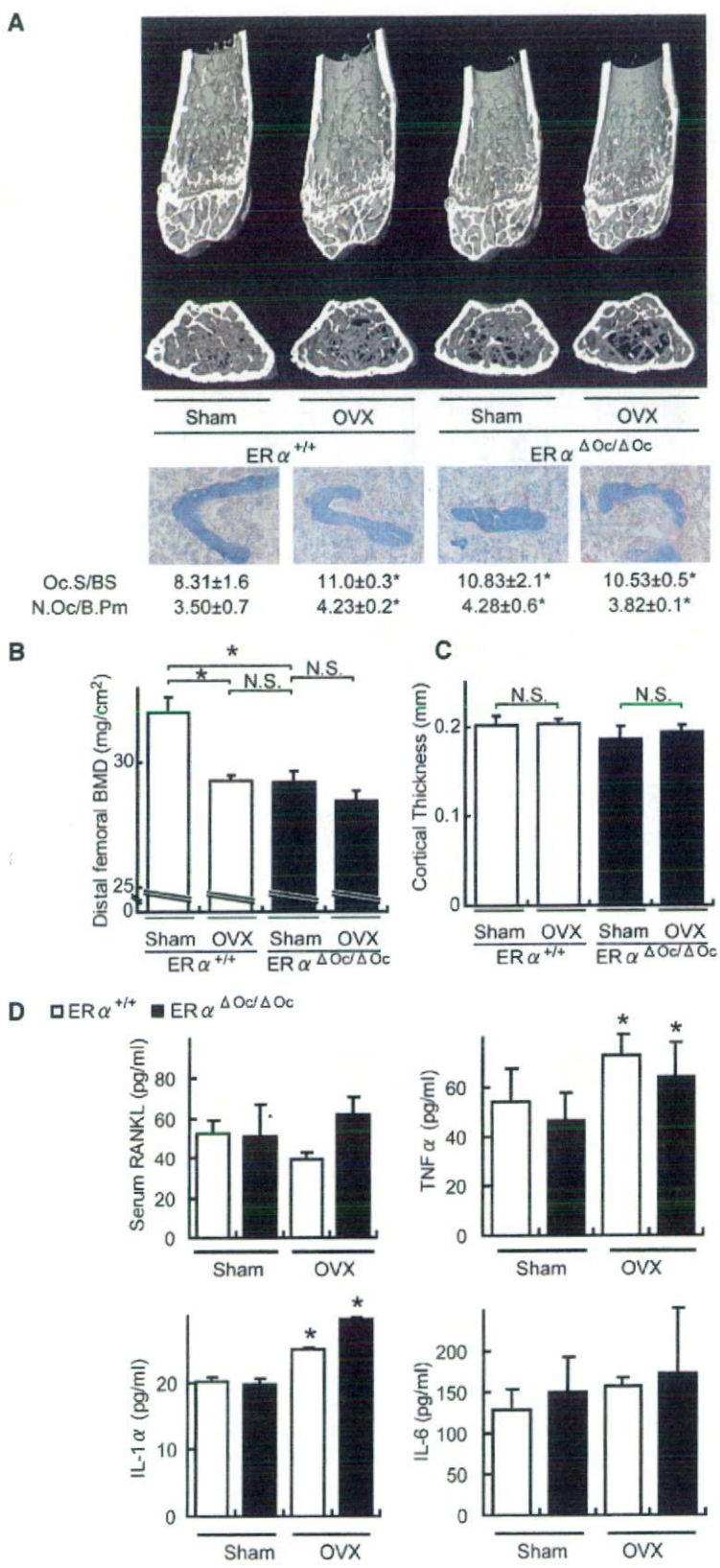


**Figure 3. No Further Bone Loss of $ER\alpha^{\Delta Oc/\Delta Oc}$ Females by Ovariectomy**

(A) Distal femoral micro CT analysis and lumbar vertebral bone histomorphometrical analysis of sham-operated or ovariectomized (OVX) 12-week-old $ER\alpha^{+/+}$ and $ER\alpha^{\Delta Oc/\Delta Oc}$ mice (*$p < 0.05$ compared to $ER\alpha^{+/+}$ sham group). Two weeks after OVX, the bone phenotype was analyzed.

(B) BMD of the distal femurs within each group are described in Figure 3A (*$p < 0.05$; N.S., not significant). Data are represented as mean ± SEM.

(C) Cortical thickness evaluation from micro CT analysis of femurs within each group described in Figure 3A. Data are represented as mean ± SEM.

(D) The levels of TNFα, IL-1α, and IL-6 in the bone-marrow cells culture media and serum RANKL (*$p < 0.05$ compared to each sham group). Data are represented as mean ± SEM.

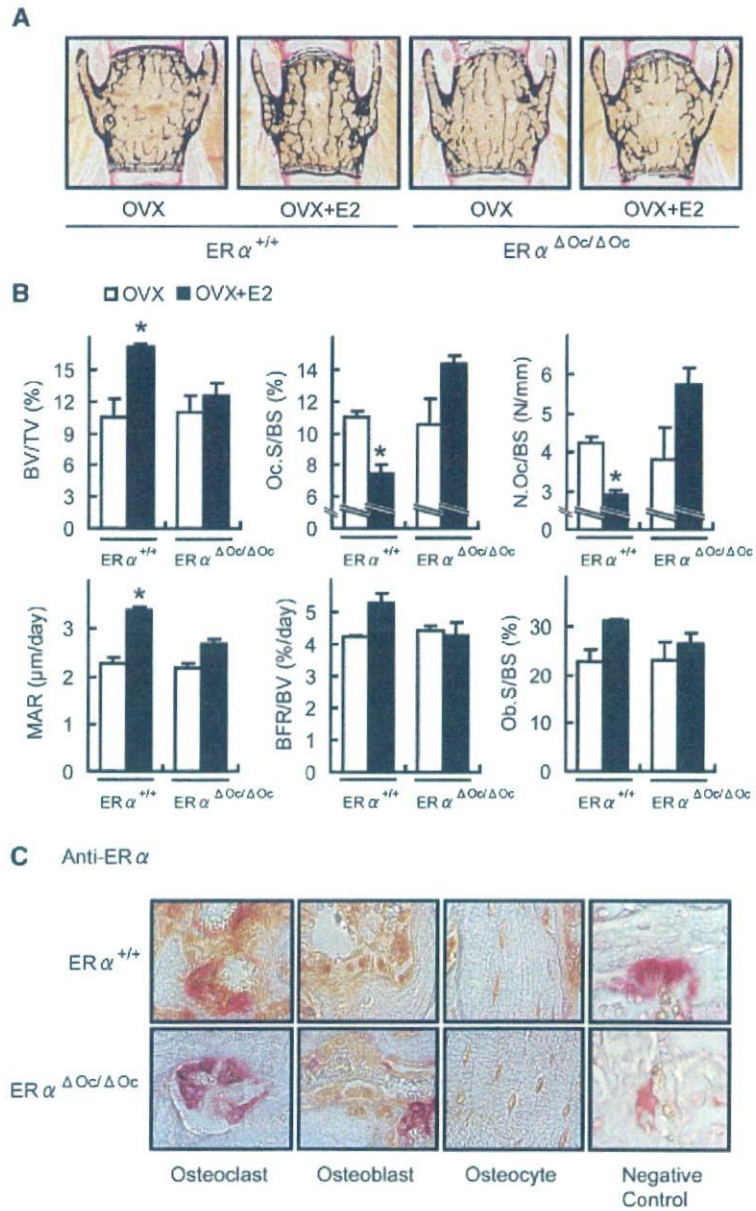


**Figure 4. Estrogen treatment failed to reverse trabecular bone loss of ovariectomized $ER\alpha^{\Delta Oc/\Delta Oc}$ females**

(A) von kossa staining of lumbar vertebral bodies of ovariectomized $ER\alpha^{+/+}$ and $ER\alpha^{\Delta Oc/\Delta Oc}$ mice treated with or without 17β-estradiol (0.83 μg/day) for 2 weeks (+E2) groups.

(B) Bone histomorphometrical analyses of the lumber vertebral bodies of 12-week-old ovariectomized $ER\alpha^{+/+}$ (left columns) and $ER\alpha^{\Delta Oc/\Delta Oc}$ (right columns) mice with (filled columns) or without (open columns) E2 treatment for 2 weeks (*$p < 0.05$ compared with E2-treated ovariectomized $ER\alpha^{\Delta Oc/\Delta Oc}$ mice). BV/TV: bone volume per tissue volume. ES/BS: eroded surface per bone surface. Oc.S/BS: osteoclast surface per bone surface. N.Oc/BS: osteoclast number per bone surface. MS/BS: mineralizing surface per bone surface. Ob.S/BS: osteoblast surface per bone surface. MAR: mineral apposition rate. BFR/BS: bone formation rate per bone surface. Data are represented as mean ± SEM.

(C) Immunochemical identification of ERα (brown) in TRAP-positive (red) differentiated osteoclasts. The femurs of 12 week-old mice were used for the immunodetection of ERα in bone cells. All labels were abolished when the primary antibody was preadsorbed with the immunizing peptide (negative control).

The number of TRAP-positive osteoclasts differentiated from the bone-marrow cells of $ER\alpha^{\Delta Oc/\Delta Oc}$ females was almost the same as that from $ER\alpha^{+/+}$ females (Figure 5A) and males (data not shown). The differentiated $ER\alpha^{\Delta Oc/\Delta Oc}$ osteoclasts had typical osteoclastic features, including the characteristic cell shape, TRAP-positive, multiple nuclei, and actin-ring formation, and were indistinguishable from the $ER\alpha^{+/+}$ osteoclasts (Figure 5B).

The expression levels of the prime osteoclastogenic transcription factors, *c-fos* and *NFATc1*, were unaltered by ERα deficiency in differentiated osteoclasts (Figure 5C). Furthermore, responses to RANKL in intracellular signaling, as represented by phosphorylation of p38 and IκB, were unaffected in $ER\alpha^{\Delta Oc/\Delta Oc}$ osteoclasts from females (Figure 5D) as well as males (data not shown). In light of these findings, it is unlikely that activated ERα in osteoclastic cells attenuates osteoclastogenesis.

## Activation of the Fas/FasL System by Estrogen in Intact Bone Is Impaired by Osteoclastic ERα Deficiency

To examine osteoclastic ERα function in intact bone, DNA microarray analysis following real-time RT-PCR of RNA from the femurs of ovariectomized $ER\alpha^{\Delta Oc/\Delta Oc}$ females treated with or without estrogen, was performed. During

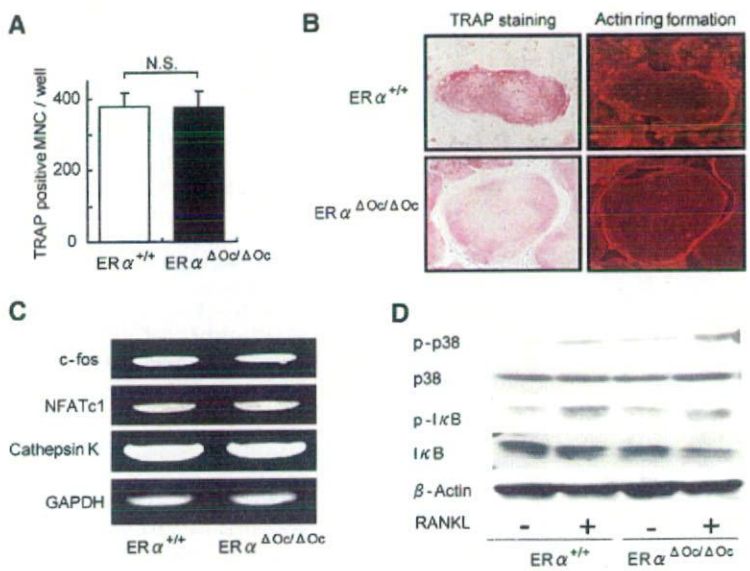


**Figure 5. ERα Deficiency Did Not Affect Osteoclastogenesis**

(A) TRAP-positive multinucleated cell count at 3 days after RANKL stimulation, cultured in 24-well plates (n = 6, N.S., not significant). Data are represented as mean ± SEM.

(B) TRAP staining and actin ring formation of RANKL induced primary cultured osteoclasts from bone-marrow cells of $ER\alpha^{+/+}$ and $ER\alpha^{\Delta Oc/\Delta Oc}$ mice.

(C) RT-PCR analysis of genes related to osteoclastogenesis.

(D) Western blot analysis of phosphorylated p38, JNK, and IκB of primary cultured bone-marrow cells stimulated with or without 100 ng/ml of RANKL for 15 min.

the search for candidate ERα target genes in bone by DNA microarray analysis (Figure S3), we found that a number of apoptosis-related factors were regulated by estrogen in the intact bone of $ER\alpha^{+/+}$ females but dysregulated in $ER\alpha^{\Delta Oc/\Delta Oc}$ females. This observation is consistent with a previous report of estrogen-induced apoptosis of mature osteoclasts (Kameda et al., 1997). Real-time RT-PCR to validate the estrogen regulations of the candidate genes revealed that gene expression of *FasL*, an apoptotic factor, was responsive to E2 (Figure 6A). Estrogen treatment (+E2) indeed induced expression of FasL protein in bone of ovariectomized $ER\alpha^{+/+}$, but this induction was not obvious in ovariectomized $ER\alpha^{\Delta Oc/\Delta Oc}$ mice (Figures 6B and 6C). Reflecting FasL induction by estrogen, estrogen-induced apoptosis (as observed by the TUNEL assay) in TRAP-positive mature trabecular osteoclasts in the distal femurs of the $ER\alpha^{+/+}$ mice was detected, but this E2 response was abolished in the $ER\alpha^{\Delta Oc/\Delta Oc}$ mice (Figure 6D). Furthermore, in mice lacking functional FasL ($FasL^{gld/gld}$), neither enhanced bone resorption nor bone mass loss was induced by ovariectomy (Figures 6E and 6F).

### Osteoclastic ERα Mediates Estrogen-Induced apoptosis by FasL

The expression level of ERα protein in differentiated osteoclasts derived from bone marrow cells was very low, but induction of *FasL* gene expression was also detectable in the cultured osteoclasts of $ER\alpha^{+/+}$ females as well as males (Figure 7A). However, this E2 response was impaired in cultured osteoclasts from $ER\alpha^{\Delta Oc/\Delta Oc}$ females (Figure 7A). It is notable that such responses are also induced by tamoxifen (Figure 7C), which is an osteoprotective SERM (Harada and Rodan, 2003). ERα overexpression augmented *FasL* gene expression in response to estrogen in cultured osteoclasts from $ER\alpha^{\Delta Oc/\Delta Oc}$ females (Figure S4A). In primary cultured calvarial osteoblasts from females as well as males (Suzawa et al., 2003), *FasL* gene induction by E2 and tamoxifen was also seen; however, it was not accompanied by increased apoptosis (data not shown). Thus, it appears that estrogen-induced apoptosis in osteoclasts is mediated by FasL expression in osteoclasts in the trabecular bone areas, presumably as well as in osteoblasts in cortical bone areas. As expected, the cell number of TUNEL-positive osteoclasts was increased by E2 in the cultured osteoclasts from $ER\alpha^{+/+}$ females, but E2-induced apoptosis was undetectable in $ER\alpha^{\Delta Oc/\Delta Oc}$ osteoclasts (Figure 7B). Consistent with FasL-induced apoptosis, *Fas* gene expression was observed (Figure 7D), but it was likely that Fas expression did not require ERα function (Figures S4B and S4C). Expression levels of *Fas* and *ERα* as well as E2 response in apoptosis appeared to fluctuate during osteoclast differentiation (Figures S4B–S4D); however, in FasL mutant ($FasL^{gld/gld}$) females, the E2-induced apoptosis was abolished (Figure S4E). These findings suggest that activated ERα in differentiated osteoclasts induces apoptosis through activating FasL/Fas signaling. This leads to suppression of bone resorption through truncating the already short life span of differentiated osteoclasts (Teitelbaum, 2006).

## DISCUSSION

Selective ablation of ERα in mature osteoclasts in female mice shows that the osteoprotective effect of estrogen is mediated by osteoclastic ERα, at least in the trabecular regions of the tibiae, femur, and lumbar vertebrae of female mice. Activated ERα by estrogen as well as SERMs appears to truncate the already short life span (estimated at 2 weeks) of differentiated osteoclasts by inducing apoptosis through activation of the Fas/FasL system.